

Scalable Spatial Stream Network (S3N) Models

Jessica P. Kunke*

Department of Mathematical Sciences, Montana State University
Julian D. Olden

School of Aquatic and Fishery Sciences, University of Washington
and

Tyler H. McCormick

Department of Statistics, University of Washington

December 16, 2025

Abstract

Understanding how habitats shape species distributions and abundances across spatially complex, dendritic freshwater networks remains a longstanding and fundamental challenge in ecology, with direct implications for effective biodiversity management and conservation. Existing spatial stream network (SSN) models adapt spatial process models to river networks by creating covariance functions that account for stream distance, but preprocessing and estimation with these models is both computationally and time intensive, thus precluding the application of these models to regional or continental scales. This paper introduces a new class of Scalable Spatial Stream Network (S3N) models, which extend nearest-neighbor Gaussian processes to incorporate ecologically relevant spatial dependence while greatly improving computational efficiency. The S3N framework enables scalable modeling of spatial stream networks, demonstrated here for 285 fish species in the Ohio River Basin ($>4,000$ river km). Validation analyses show that S3N accurately recovers spatial and covariance parameters, even with reduced bias and variance compared to standard SSN implementations. These results represent a key advancement toward large-scale mapping of freshwater fish distributions and quantifying the influence of environmental drivers across extensive river networks.

Keywords: SSNs, spacetime processes, ecology, networks, computational efficiency

*The authors gratefully acknowledge the following sources of funding: J.D.O. was supported by the Richard C. and Lois M. Worthington Endowed Professor in Fisheries Management from the School of Aquatic and Fishery Sciences, University of Washington.

1 Introduction

Freshwater ecosystems are among the most diverse on Earth, providing essential benefits such as fisheries, clean drinking water, material resources, and cultural value to billions of people (Lynch et al. 2023). Despite covering a small fraction of the planet’s surface, fresh waters also support roughly 12% of all described animal species, including nearly one-third of all vertebrates (Darwall et al. 2018). However, freshwater biodiversity is facing severe and accelerating declines—vertebrate populations in freshwater ecosystems are decreasing at nearly four times the rate of those in marine or terrestrial environments and have greater projected extinction rates in the future (Tickner et al. 2020, Urban 2024). Species face intense pressure from a wide range of persistent and emerging threats, including climate change, land-use modification, pollution, invasive species, infectious diseases, algal blooms, flow alteration, over-exploitation, salinization, and contaminants such as pesticides, microplastics, and pharmaceuticals (Reid et al. 2019). To facilitate management interventions that can effectively curtail or even reverse the decline in freshwater biodiversity, research must continue to address key knowledge gaps that, at present, impede progress (Tickner et al. 2020, Harper et al. 2021).

A central challenge in freshwater ecology is to predict how present and future habitat conditions influence species distributions and population abundances, and to apply these insights to inform effective fisheries management (Paukert et al. 2021). Modeling the distribution of freshwater fishes involves various approaches that seek to capture the complex interplay between environmental conditions, biotic interactions and the spatial structure of rivers that is unique to freshwater ecosystems. Species distribution models are widely used to predict suitable habitats by correlating species occurrences with environmental variables (e.g., Bond et al. 2011, Markovic et al. 2012, Radinger et al. 2017), in addition to accounting for species interactions (e.g., Wagner et al. 2020). More spatially explicit methods, such as

network-based and graph-theoretical models, consider the dendritic structure of river systems and the effects of connectivity on fish distributions (Erős et al. 2012). Process-based and individual-based models simulate ecological dynamics like dispersal, reproduction, and survival, offering a mechanistic view of species responses to changing conditions (Rogosch et al. 2019, Tonkin et al. 2021). The choice of model depends on the research question, spatial grain and extent, data availability, computation limitations, and the desire to incorporate river network structure and the contributing upstream watershed.

Modeling fish distributions in river networks at large spatial scales presents several significant challenges. Rivers are organized into hierarchical dendritic networks embedded within the terrestrial landscape, where organisms respond to a combination of biotic and abiotic factors that vary spatially (Jackson et al. 2001, Olden et al. 2010, Tonkin et al. 2018). While seminal research focused on rivers' linearity (Vannote et al. 1980), viewing them as branched structures offers a more robust understanding of the spatial dynamics shaping riverine biodiversity (Fausch et al. 2002, Campbell Grant et al. 2007, Altermatt 2013), supporting more robust management and conservation practices. With this greater understanding comes the necessity of accounting for spatial dependence in models of fish distributions.

Spatial regression models, such as kriging or Gaussian processes, model a response variable such as species abundance as a function of environmental factors, capturing remaining spatial dependence through some spatial process (Rasmussen & Williams 2006, Cressie & Wikle 2011). Spatial dependence among observations along a river network is a function not only of Euclidean distance, common to most spatial process models, but also of the directed or undirected distance along the stream network (Dent & Grimm 1999, Wyatt 2003, Ganio et al. 2005, Peterson et al. 2006, Webster et al. 2008). For instance, waterborne chemicals may passively flow downstream, larval invertebrates drift downstream, and fish can actively

swim downstream or upstream at rates that vary depending on the species (e.g., [Bilton et al. 2001](#), [Schofield et al. 2018](#), [Leibowitz et al. 2018](#), [Comte & Olden 2018](#)). Though it may seem natural to simply replace one distance metric with the other, substituting stream distance for Euclidean distance in already established covariance functions does not guarantee a valid (positive definite) covariance function ([Ver Hoef et al. 2006](#)). To address this challenge, [Ver Hoef & Peterson \(2010\)](#) developed valid stream covariance functions using moving-average constructions and proposed spatial stream network (SSN) models to incorporate these covariance functions. SSN models were made available first as an ArcGIS toolkit and an R package ([STARS](#) and [SSN](#)) in 2014 and later as a pair of R packages ([SSNbler](#) and [SSN2](#)) in 2024 ([Peterson & Ver Hoef 2014](#), [Ver Hoef et al. 2014](#), [Peterson et al. 2024](#), [Dumelle et al. 2024](#)). SSN models revolutionized how scientists model ecological processes and organisms in river networks.

While SSN models represent a significant advance in handling the spatial dependence induced by stream networks, they are also known to be computationally expensive. Given n locations at which observations are available, fitting spatial process models requires $O(n^3)$ floating point operations (flops) and $O(n^2)$ storage to compute the inverse and determinant of the $n \times n$ covariance matrix ([Rasmussen & Williams 2006](#), [Datta et al. 2016b](#)). Fitting SSNs additionally requires computing pairwise stream distances and other network information in order to compute covariances; we and previous authors refer to this as preprocessing, as these steps are necessary before fitting a model. While computing the Euclidean distance between two points requires only their Cartesian coordinates, computing the stream distance between two points requires knowledge of stream network structure between the two points: for instance, does water flow directly from one point to another, or does water flow from both points to meet at some common junction further downstream? Computing these path lengths requires knowledge of how different river segments, called **reaches**, are

connected. The computational expense increases with the number of reaches and observation locations. Even for a fixed number of reaches, the depth and branching structure of the network can affect the computational cost of computing stream distances and other network information.

The scale and computational time of existing studies using SSNs illustrate the computational demands of these models. In a study of the Salt River watershed on the Idaho-Wyoming border, [Isaak et al. \(2017\)](#) examined a single taxon (trout) based on 108 observations collected over a 2,300-km² area. In a subsequent study, [Isaak et al. \(2020\)](#) applied SSNs to two species, each with 2,000-3,000 observations over a 90,822-km² area. Fitting the model required five days of computation time with the older `SSN` R package and “some model fits [...] completed in approximately 10 minutes” with the newer `S3N` R package, results which are consistent with our own benchmarking presented in the current paper. However, with twice or tenfold the number of observations or more stream reaches, both of which reflect the data we study in this paper, estimation quickly becomes infeasible.

In this paper, we develop the scalable spatial stream network (S3N) model, which enables larger-scale (such as regional and national) spatial process models on stream networks by extending nearest-neighbor Gaussian processes to a stream context, identifying essential preprocessing steps, and implementing the preprocessing more efficiently. We provide a detailed description of the S3N model (Section 2), followed by a demonstration that S3Ns provide essential computational gains over existing models without compromising accuracy, permitting the analysis of larger networks with more observations (Section 3). Next, we apply the S3N model to estimate the geographical distributions, local (reach-scale) densities, and total population sizes for 8,924 observations of 285 fish species across the Ohio River Basin, one of the most species-rich river systems in North America with diverse ecological habitats (Section 4). Lastly, we summarize the findings and limitations of this study and

highlight directions for future work (Section 5).

2 Scalable spatial stream network models (S3Ns)

Let $Y = (Y(s_1), \dots, Y(s_n))$ be the observed fish densities (the number of fish per 100-m length of river) at n point locations s_1, \dots, s_n along a stream network. Given these fish densities, we wish to estimate the response variable across the entire regional stream network and estimate region-wide summary statistics. The fundamental basis for the S3N model is a Gaussian process model, under which Y has a multivariate normal distribution whose mean is a linear function of p covariates (represented in matrix form as X with coefficients β) and whose covariance is given by a covariance function Σ (Rasmussen & Williams 2006, Cressie & Wikle 2011):

$$\begin{aligned} Y &= X\beta + w, \quad w \sim N(0, \Sigma), \\ \Sigma(s_i, s_j) &= C(s_i, s_j) + \tau^2 \delta_{ij}. \end{aligned} \tag{1}$$

Here $\tau^2 \delta_{ij}$ captures any independent error, whether from measurement error or from variation at scales smaller than the distances between observations, and $C(s_i, s_j)$ represents the spatial covariance. Outside the stream context, $C(s_i, s_j)$ is often parameterized as a function of the Euclidean distance between the two points: $C(s_i, s_j) = C_e(s_i, s_j \mid \theta_e)$, where θ_e represents the parameters of this function.

Our S3N model modifies the nearest-neighbor Gaussian process model, an approximation of the Gaussian process model, for river networks by selecting nearest neighbors based on

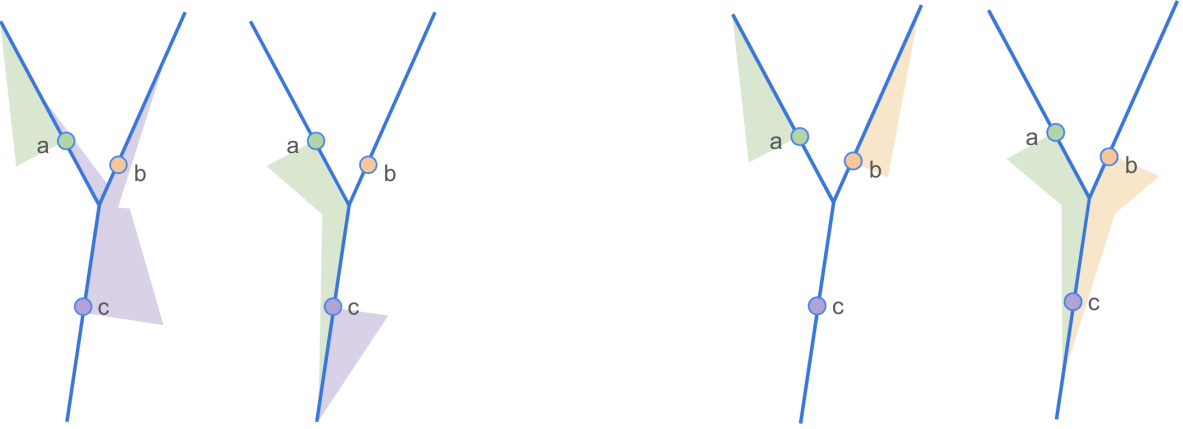
stream distance and including covariance components that are functions of stream distance:

$$\begin{aligned}
Y &= X\beta + w, \quad w \sim N\left(0, \tilde{\Sigma}\right), \\
w(s_i) \mid w(M(s_i)) &\sim N(a_i, d_i), \\
a_i &= \Sigma(M(s_i), M(s_i))^{-1} \Sigma(M(s_i), s_i), \\
d_i &= \Sigma(s_i, s_i) - \Sigma(s_i, M(s_i)) a_i, \\
\Sigma(s_i, s_j) &= \pi_{ij} C_u(s_i, s_j \mid \theta_u) + C_d(s_i, s_j \mid \theta_d) + C_e(s_i, s_j \mid \theta_e) + \tau^2 \delta_{ij}.
\end{aligned} \tag{2}$$

We provide details on each of the model components in subsequent sections. Section 2.1 details the stream covariance components C_u and C_d . Section 2.2 explains the nearest-neighbor Gaussian process, which accounts for the approximation of the covariance matrix Σ by $\tilde{\Sigma}$ in our model (2) above, as well as the conditioning of the spatial process $\omega(s_i)$ on only nearest neighbors $M(s_i)$. This nearest-neighbor approximation reduces the computational cost of estimation from $O(n^3)$ to $O(n)$, where n is the number of observation points. Sections 2.3 and 2.4 cover inference and prediction, respectively. Section 2.5 describes S3N preprocessing and why it is more efficient than SSN preprocessing.

2.1 Stream-based covariance

Stream flow can induce spatial covariance patterns that are not accounted for by Euclidean distance alone. Pollutants and most invertebrate larvae tend to move with the flow of water, and fish can swim with or against the flow. Starting with [Cressie et al. \(2006\)](#) and [Ver Hoef et al. \(2006\)](#), Gaussian process models have been adapted to incorporate flow-induced correlations into the covariance function $C(s_i, s_j)$. Substituting stream distance for Euclidean distance in existing covariance functions such as the Matérn or the spherical covariance functions does not guarantee a positive definite covariance matrix ([Ver Hoef et al. 2006](#)). Instead, [Ver Hoef & Peterson \(2010\)](#) construct valid stream covariance functions using the approach from [Yaglom \(1987\)](#) and [Ver Hoef & Barry \(1996\)](#) of convolving moving



(a) Flow-connected points a and c .

(b) Flow-unconnected points a and b .

Figure 1: Tail-up (left of each panel) and tail-down (right of each panel) covariances for (a) flow-connected and (b) flow-unconnected points. Adapted from [Ver Hoef et al. \(2019\)](#).

average functions $g(\cdot | \theta)$ with a white noise process $W(\cdot)$:

$$Z(s | \theta) = \int_{-\infty}^{\infty} g(x - s | \theta) dW(x).$$

[Ver Hoef & Peterson \(2010\)](#) develop two classes of covariance functions, which they refer to as tail-up and tail-down. For tail-up covariance functions, the moving average function is non-zero only upstream of the point in question, while for tail-down covariance functions, the moving average function is non-zero only downstream of the point in question. As shown in Figure 1, we can visualize this as a shaded region alongside each stream reach, where the width of the region at each point along the stream is proportional to the magnitude of the moving average function at that point along the reach. Visualized this way, the names tail-up and tail-down correspond to whether the “tails” of the shaded regions (and to an extent, the tails of the swimming fish, as we see in the next paragraph) point upstream or downstream.

Spatial correlation between two points occurs if and only if their moving average functions

overlap:

$$C(s_i, s_j | \theta) = \text{Cov}(Z(s_i | \theta), Z(s_j | \theta)) = \int_{-\infty}^{\infty} g(x - s_i | \theta)g(x - s_j | \theta)dx.$$

As a result, spatial dependency with tail-up covariance occurs between two points only if the stream flows from one point to the other (flow-connected points), while both flow-connected and flow-unconnected pairs of points can be spatially correlated with tail-down covariance (see Figure 1). Tail-up models are therefore useful for modeling waterborne chemicals and small organisms that move passively with the stream flow, as well as fish that can swim more easily downstream.

As in existing SSNs, S3N models include these stream covariance components as additive components. In this work, we focus on the tail-up component of the latent covariance since this term accounts for downstream flow and is therefore likely to capture more of the remaining spatial correlation in the fish survey data after including relevant covariates. Tail-down and Euclidean components may be implemented in the S3N model in future work; we discuss considerations for these additions in Section 5. Also as in existing SSNs, we multiply the tail-up covariance function by spatial weights π_{ij} that account for the proportional influence of confluent stream segments; see [Ver Hoef & Peterson \(2010\)](#) and [Ver Hoef et al. \(2019\)](#) for further details.

2.2 Computationally efficient estimation

Estimating the parameters of a Gaussian process model requires storing the covariance matrix and computing its inverse and determinant. The full covariance matrix for estimation with n observation point locations is $n \times n$. Computing the full likelihood for estimation therefore requires $O(n^2)$ storage, and computing the inverse and determinant of the covariance matrix using the Cholesky decomposition requires $O(n^3)$ floating point operations (flops). Estimation with these models becomes prohibitive on personal computers as n

grows beyond 10^4 (Rasmussen & Williams 2006, Datta 2022).

To make estimation feasible over river networks with many observations and reaches, we adapt nearest-neighbor Gaussian processes (NNGPs) to stream networks. Many different methods have been developed to provide fast approximations of spatial process models. We focus on nearest-neighbor Gaussian processes since these extend the approximation into valid generative models in their own right, enabling prediction at arbitrary locations aside from the observations; further details are provided below. Additionally, the nearest-neighbor approximation is consistent with the idea that populations of fish typically have some finite geographic range that is relevant to them during their lifetimes.

NNGPs are based on sparse nearest-neighbor approximations. The full likelihood—the joint probability of the values of the Gaussian process at all observation and prediction points—can be expressed as a product of conditional densities using the general product rule:

$$\begin{aligned}
p(Y) &= p(Y(s_1)) \cdot p(Y(s_2) | Y(s_1)) \cdot p(Y(s_3) | Y(s_2), Y(s_1)) \cdots \\
&\quad p(Y(s_n) | Y(s_{n-1}), \dots, Y(s_1)) \\
&= p(Y(s_1)) \prod_{i=2}^n p(Y(s_i) | Y(H(s_i))), \tag{3}
\end{aligned}$$

where $H(s_i) := \{s_{i-1}, \dots, s_1\}$ is the conditioning set for s_i and $Y(H(s_i))$ is the vector of responses (fish densities, in our case) at the locations in $H(s_i)$. Equation 3 holds for any ordering of the locations s_i . Vecchia (1988) proposed approximating the likelihood by conditioning each point on at most some fixed number m of its nearest neighbors, replacing $H(s_i)$ with a subset $M(s_i) \subseteq H(s_i)$ of m or fewer points that are nearest to s_i by Euclidean distance. Specifically, for $i \leq m$, $M(s_i) = H(s_i)$ and $|M(s_i)| = i \leq m$. For $i > m$, $M(s_i)$ is the set of m nearest neighbors by Euclidean distance to s_i , and $|M(s_i)| = m$. The

resulting likelihood approximation is

$$p(Y) \approx p(Y(s_1)) \prod_{i=2}^n p(Y(s_i) | Y(M(s_i))). \quad (4)$$

This approximate likelihood only requires storing and computing n matrices of size at most $m \times m$, reducing storage from $O(n^2)$ to $O(nm^2)$ and computational cost in flops from $O(n^3)$ to $O(nm^3)$.

A limitation of likelihood approximation methods such as that of [Vecchia \(1988\)](#) in Equation 4 above is that they define an approximation at the observed locations; they do not necessarily allow us to predict values at other locations unless they are shown to correspond to some underlying process. The main alternative class of approaches, low rank models, are still too computationally expensive for large n and perform poorly in the presence of high spatial correlation, both of which are critical for regression on large spatial datasets ([Stein 2014](#), [Datta et al. 2016a](#)).

[Datta et al. \(2016a\)](#) proved that the nearest-neighbor approximation of [Vecchia \(1988\)](#) corresponds to a process of its own. Thus, the Vecchia approximation yields a new Gaussian process model with covariance matrix $\tilde{\Sigma} := (I - A)^{-1} D (I - A)^{-T}$ which approximates the original Gaussian process. The Cholesky factor of $\tilde{\Sigma}$, $\tilde{L} = D^{-1/2} (I - A)$, requires only $O(nm^3)$ flops and $O(nm^2)$ storage, compared to $O(n^3)$ flops and $O(n^2)$ storage for the Cholesky factor of the covariance matrix for the full original process.

The NNGP model of [Datta et al. \(2016a\)](#) is given by

$$\begin{aligned} Y &= X\beta + w, \quad w \sim N(0, \tilde{\Sigma}), \\ w(s_i) | w(M(s_i)) &\sim N(a_i, d_i), \\ a_i &= \Sigma(M(s_i), M(s_i))^{-1} \Sigma(M(s_i), s_i), \\ d_i &= \Sigma(s_i, s_i) - \Sigma(s_i, M(s_i)) a_i, \\ \Sigma(s_i, s_j) &= C_e(s_i, s_j | \theta_e) + \tau^2 \delta_{ij}. \end{aligned} \quad (5)$$

NNGPs dramatically improve the computational scalability of Gaussian process models, but to our knowledge, they have not yet been implemented for distance measures other than Euclidean distance. The distance measure affects both which neighbors are nearest and how the covariance function is defined. Whereas [Vecchia \(1988\)](#) and [Saha & Datta \(2018\)](#) choose the neighbor sets $M(s_i)$ to be the m nearest neighbors of s_i among s_1, \dots, s_{i-1} with respect to Euclidean distance, we instead choose these neighbor sets based on stream distance, and we include covariance components based on stream distance, leading to the S3N model shown in (2).

2.3 Inference

Estimation and inference for NNGP models can be performed using Bayesian or frequentist methods. The `spNNGP` R package provides full posterior distributions using MCMC, while the `BRISC` R package (named after a bootstrap method by the same name, described below) estimates parameter values using maximum likelihood estimation and estimates their confidence intervals using a bootstrap since MLE asymptotic guarantees are limited in the infilling asymptotic paradigm typical of many spatial problems. [Saha & Datta \(2018\)](#) demonstrate that `BRISC` is much faster than `spNNGP` for both estimation and prediction while providing comparable accuracy. Since our primary goal is scalability, we implement S3N models within a frequentist inferential framework. Our estimation code is built upon the existing `BRISC` R package ([Saha & Datta 2018](#)), which uses efficient numerical linear algebra algorithms for matrix and vector computation as described by [Finley et al. \(2022\)](#). The `BRISC` package is also implemented primarily in C with calls to the Fortran LAPACK library. All these features contribute to reducing the computational cost of estimation, inference and prediction with the S3N model.

Confidence intervals for the fixed effect parameters in both our S3N model and existing

SSNs can be obtained for free during estimation as $\left(X^T \hat{\Sigma}^{-1} X\right)^{-1}$. However, the Bootstrap for Rapid Inference on Spatial Covariances—or BRISC (Saha & Datta 2018), after which the BRISC package is named—allows for the estimation of confidence intervals for covariance parameters as well, a feature that is not currently available in SSNs. BRISC is a clever, more computationally efficient adaptation of a parametric bootstrap proposed by Olea & Pardo-Igúzquiza (2011), in which the data are decorrelated before sampling and recorrelated afterward by multiplication with either the Cholesky factor or its inverse.

2.4 Regional estimates using prediction

Estimating fish abundance over an entire region based on observed values requires prediction at unobserved locations. Given observations $Y_1 = (Y(s_1), \dots, Y(s_n))$ at a set of locations $\mathcal{D}_1 = \{s_1, \dots, s_n\}$ with covariates X_1 , we wish to predict the response process $Y_2 = (f(r_1), \dots, Y(r_k))$ at another set of locations $\mathcal{D}_2 = \{r_1, \dots, r_k\}$ with covariates X_2 in order to map fish abundance across the region of interest and estimate regional population sizes. Let $\Sigma_{11} := \text{Cov}(Y_1, Y_1)$, $\Sigma_{12} := \text{Cov}(Y_1, Y_2)$, and so on; then the joint distribution of Y_1 and Y_2 under a Gaussian process is

$$\begin{bmatrix} Y_1 \\ Y_2 \end{bmatrix} \sim N \left(\begin{bmatrix} X_1 \\ X_2 \end{bmatrix} \beta, \begin{bmatrix} \Sigma_{11} & \Sigma_{12} \\ \Sigma_{21} & \Sigma_{22} \end{bmatrix} \right), \quad (6)$$

and the conditional distribution of Y_2 given Y_1 , X_1 and X_2 is

$$Y_2 | Y_1, X_1, X_2 \sim N(M, Q), \text{ where} \quad (7)$$

$$M = X_2 \beta + \Sigma_{21} \Sigma_{11}^{-1} Y_1, \quad Q = \Sigma_{22} - \Sigma_{21} \Sigma_{11}^{-1} \Sigma_{12}. \quad (8)$$

In the S3N model, as in the original NNGP model, the matrix inverse Σ_{11}^{-1} is approximated using the sparse Cholesky factor.

2.5 Computationally efficient preprocessing

We reduce the computational cost of model preprocessing by identifying the fundamental preprocessing steps and implementing them with minimal overhead. Computing stream distances requires the adjacency matrix of stream reaches in the stream network, which involves comparing the downstream node of each reach with the upstream nodes of other reaches. This can be accomplished by uniquely identifying the reach upstream and downstream nodes as entities distinct from the reaches themselves, mapping reaches to their corresponding upstream and downstream nodes, and then mapping downstream nodes of each reach to upstream nodes of other reaches. Computing pairwise stream distances between observation or prediction points in the network also requires the length of each reach and where each point on the stream network is located relative to the endpoints of the reach containing it.

In our implementation of S3N models, we use the `sf` R package to extract the coordinates of the upstream and downstream endpoints or nodes of each stream reach ([Pebesma 2018](#), [Pebesma & Bivand 2023](#)). Each stream reach is represented as one or more line segments in series, and the streams data frame has a geometry column containing all the endpoints of the line segments that make up each stream reach, so we extract the upstream and downstream node coordinates for all reaches in parallel and add them as new columns to the data frame. We then use the coordinate pair of each upstream or downstream node, pasted together as a string, as the unique identifier of that node. This provides an edge list from which we can compute the stream reach adjacency matrix using the `igraph` R package ([Csárdi & Nepusz 2006](#), [Antonov et al. 2023](#), [Csárdi et al. 2025](#)), avoiding the computation of pairwise Euclidean or stream distances until they are needed. For row-wise computations, we use vectorized R functions instead of for loops, and we avoid creating additional objects by embedding as much of this additional stream network information

into the streams data frame as possible.

By contrast, existing implementations of SSNs have less direct ways of identifying the network structure. Both implementations of the SSN preprocessing—as the **STARS** ArcGIS toolkit in 2014, which consists of a set of Python scripts, and as the **SSNbler** R package in 2024—are a computational bottleneck in the application of SSN models as network size increases. In **STARS**, the first preprocessing step of building the stream network includes a nested loop over reaches that dominates the runtime for this step, rendering it $O(r^2)$ where r is the number of reaches. There are a number of other unnecessary loops and steps that increase runtime even if the nested loop were vectorized. Rather than computing an adjacency matrix, **SSNbler** computes pairwise Euclidean distances between all upstream nodes and all downstream nodes in order to identify which stream reaches are connected, which makes the computational cost at least $O(r^2)$. Therefore, an essential step we take to make SSNs scalable is to identify the fundamentally required preprocessing steps, implement them efficiently, and avoid as many additional expensive steps as possible. Section 3 compares the computational costs of preprocessing in the S3N model to those of SSNs.

3 Evaluating computational efficiency and accuracy

We present the results of benchmarking and validating S3Ns against existing SSNs using the newest implementation of SSN preprocessing (**SSNbler**) and model fitting (**SSN2**) in RStudio using the R function `system.time()`. We also benchmarked S3N preprocessing against the older preprocessing implementation, the **STARS** ArcGIS toolkit; a brief summary is provided at the end of Section 3.2, and further details and results are available in the supplementary materials.

In our benchmarking analysis, we sought to fairly and robustly compare S3Ns and SSNs by matching steps with similar purposes (details are provided in the supplementary materials),

but we acknowledge that some of the steps of one method may include tasks that appear elsewhere in the other code, or implementation-specific tasks that appear nowhere in the other code. We could instead have extracted more specific tasks from each model, but this would require recoding some of the implementations (for instance, extracting just the components of a function that do particular tasks even if that task is not currently available as its own function), and since our main purpose was to determine the practical computational expense of each approach, we left the implementations intact. We experimented with both approaches and found that they ultimately lead to similar findings.

3.1 Setup

For benchmarking and validating S3Ns versus SSNs, we chose six nested stream networks of increasing size, ranging from 284 to 169,092 stream reaches. These networks are shown in Figure 2 and details are presented in Table 1. The largest of the six networks is the Ohio River Basin, also known as Hydrologic Unit Code 5 by the United States Geological Survey (USGS). We used the flowline and prediction point shapefiles from the National Stream Internet (NSI), which spans streams across the United States ([Nagel et al. 2017](#)); these flowlines are high-resolution digital maps of streams that were developed for use with spatial stream network models to ensure that topological assumptions of the spatial stream network models are met.

For prediction points, we used the midpoint of every reach in the network except for any short reaches that were added to correct topological issues in the network, making the number q of prediction points for each network slightly less than the number of reaches. For observation locations, we drew a random sample of size $n = \min(\text{ceiling}(q/2), 10000)$ of the prediction points. For each network, we simulated responses at the observation points from the following SSN model with exponential tail-up covariance and two fixed effects, an

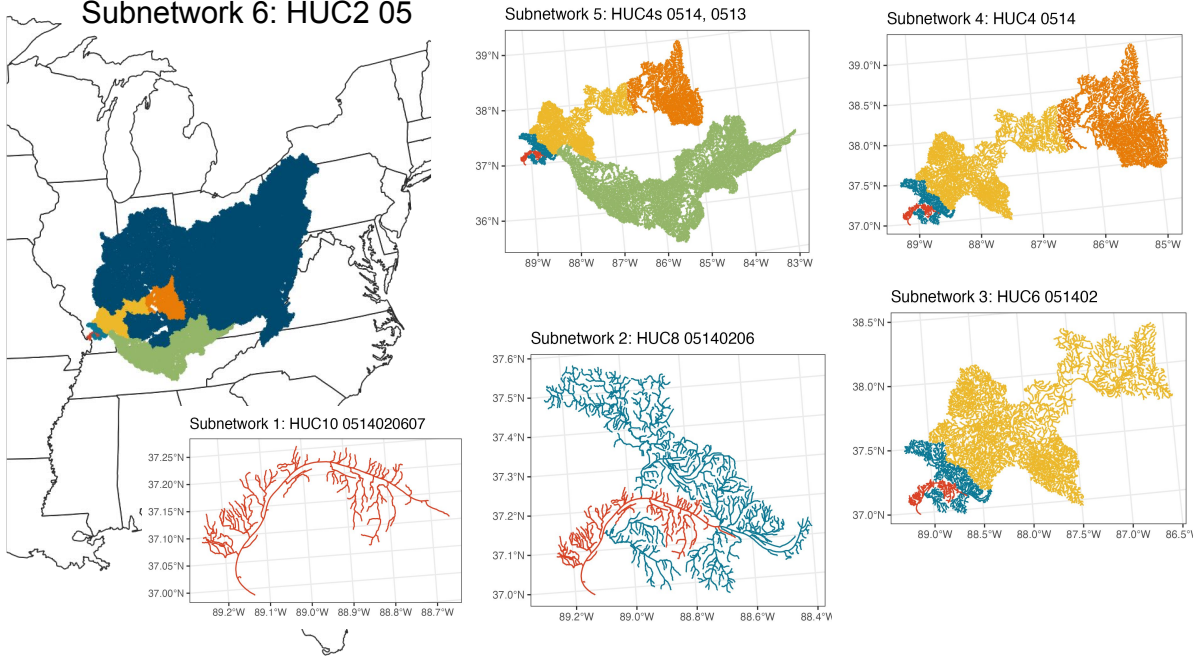


Figure 2: The six subnetworks of the Ohio River Basin used for benchmarking. Network i is a subnetwork of Network $i + 1$ for $i = 1, \dots, 5$. Networks 1-3 were also used for model validation.

intercept β_0 and a single covariate β_1 :

$$Y = X\beta + w, \quad w \sim N(0, \Sigma), \quad (9)$$

$$\Sigma(s_i, s_j) = \pi_{ij}\sigma^2 \exp(-h_{ij}/\lambda) + \tau^2\delta_{ij}.$$

It is worth emphasizing that we simulate the data from an SSN model, which makes no nearest-neighbor approximations. Here, τ^2 is the independent variance, σ^2 is the exponential tail-up spatial variance scaling parameter, and λ is the range parameter representing the characteristic distance for spatial correlations. We simulated from this model with $\beta_0 = 0.5$, $\beta_1 = -44$, $\tau^2 = \sigma^2 = 5$, and $\lambda = 0.1$.

For both S3N and SSN, we simulated 50 datasets from this model for each of the three smallest networks and 10 for Network 4, and we benchmarked each model once on each dataset; we refer to these simulated datasets as replications. For Network 5, we used 10

Table 1: Description of benchmark networks and the number of replications used to benchmark S3Ns and SSNs on each network. Only 2 replications were used for SSNs on Network 5 because of the longer runtime required by the SSN preprocessing package **SSNbler**. **SSNbler** crashed on Network 6. Predictions were made at the midpoint of every reach in the network including at points where observations were simulated, except for any short reaches that were added to correct topological issues in the network, making the number of prediction points for each network slightly less than the number of reaches. For observation locations, we drew a random sample of the prediction points and simulated fish counts from an SSN model.

		# Points		# Replications	
Network	# Reaches	Prediction	Observation	S3N	SSN
1	284	283	142	50	50
2	1,273	1,267	634	50	50
3	7,146	7,123	3,562	50	50
4	11,540	11,515	5,758	10	10
5	30,748	30,698	10,000	10	2
6	169,092	168,875	10,000	10	NA

replications for S3N but only ran SSN on the first two of those replications due to the longer runtime and higher memory requirements. **SSNbler** crashed on Network 6, but we benchmarked S3N with 10 replications. For the three smallest networks, we completed S3N and SSN preprocessing, pairwise distances, and estimation on every replication, while for the three largest networks we performed only the preprocessing steps. Therefore, we use all six networks for benchmarking and the three smallest networks for validation.

3.2 Benchmarking results

Benchmarking results between S3N and **SSNbler** are summarized in Figure 3. Running **SSNbler** on Network 5 required increasing the memory limit in RStudio, and **SSNbler** failed on Network 6 due to integer overflow while computing pairwise Euclidean distances between all upstream nodes and all downstream nodes in order to identify which stream reaches are connected. While this is not a fundamental preprocessing step, it is part of the implementation of **SSNbler**. On Network 5, the runtime for each of the three preprocessing steps was greater for **SSNbler** than S3N by a factor of 50-200. Additionally, SSN required over 48 GB memory while preprocessing Network 5. The runtime for building the stream network with the **SSNbler** code appears to grow at a rate of at least $O(r^3)$ where r is the number of reaches. By contrast, based on our empirical findings, building the stream network with S3N is approximately linear in r .

Consistent with previous theoretical and empirical findings on SSNs and NNGPs, our results suggest that estimation is $O(n^3)$ for the SSN model and $O(n)$ for the S3N model. On Network 3, the largest model for which we benchmarked estimation as well as preprocessing, estimation required only 0.83 seconds for S3N compared to 912.45 seconds (15.3 minutes) with SSN. The total computation time including preprocessing, computing pairwise distances, and estimating the model was 2.02 minutes for S3N, of which 1.78 minutes was devoted to computing pairwise distances, and 19.7 minutes for SSN. Computing pairwise distances for S3N can be made more efficient by rewriting the code in base R or C and by using a smart search for nearest neighbors; see Section 5 for further details.

We also benchmarked S3N preprocessing against the **STARS** ArcGIS toolkit. One of the first steps of **STARS** preprocessing, the Polyline to Landscape tool, required about 4 hours on Network 6, while the analogous steps in S3N preprocessing took about 1 minute. Further details are provided in the supplementary materials.

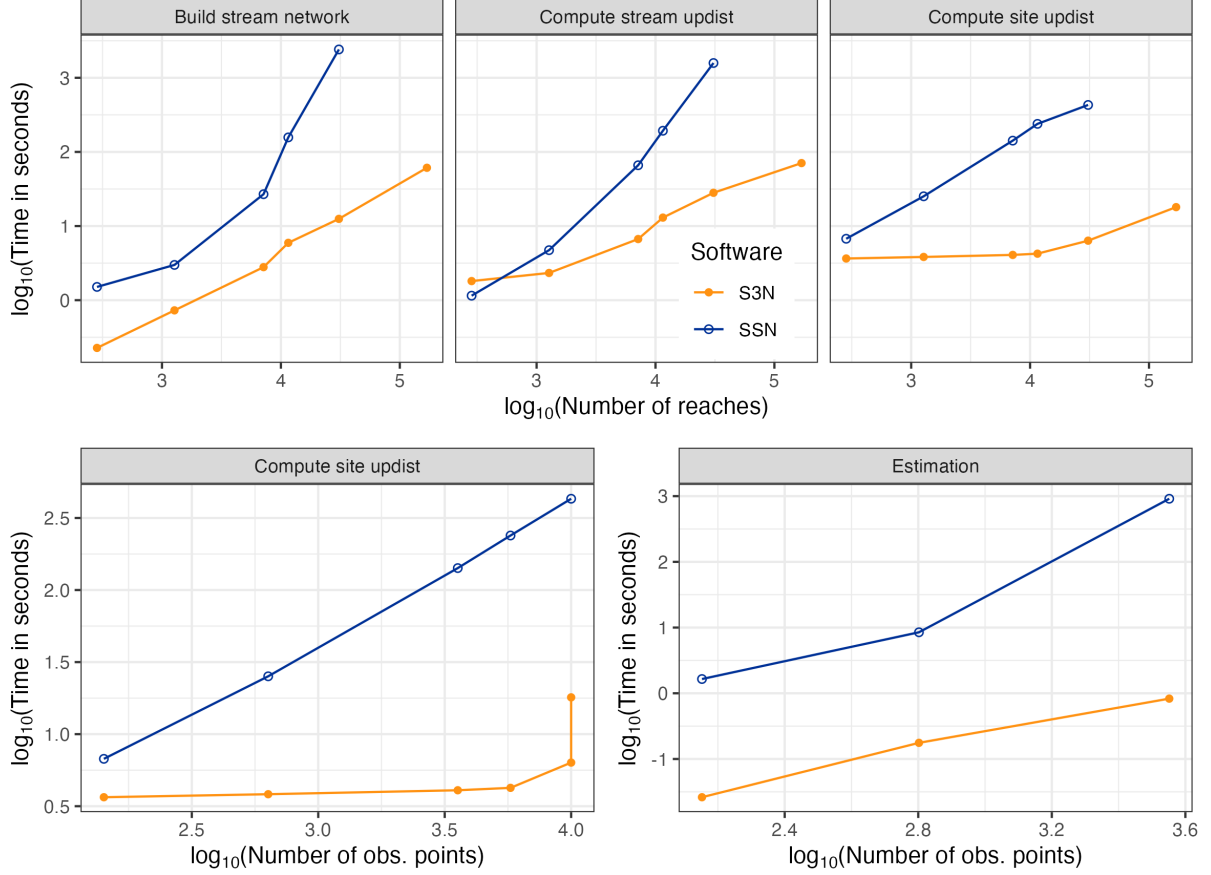


Figure 3: Benchmarking results for S3N and SSN preprocessing. Note that for the largest network size (number of reaches) tested here, `SSNbler` failed while building the stream network and is therefore not shown here. Runtimes for computing site upstream variables depend not only on (a) the number of reaches but (b) the number of observation sites and are therefore shown as a function of each of these network properties. Estimation times were computed for Networks 1-3, and preprocessing times were computed for Networks 1-6.

3.3 Validation results

We validated S3N against SSN models on Networks 1-3 using data simulated from the SSN in Equation (9). The patterns are similar across the three networks, so we present our interpretation of Network 3 and provide results for the other two networks in the supplementary materials. Figure 4 compares S3N and SSN parameter estimates on Network

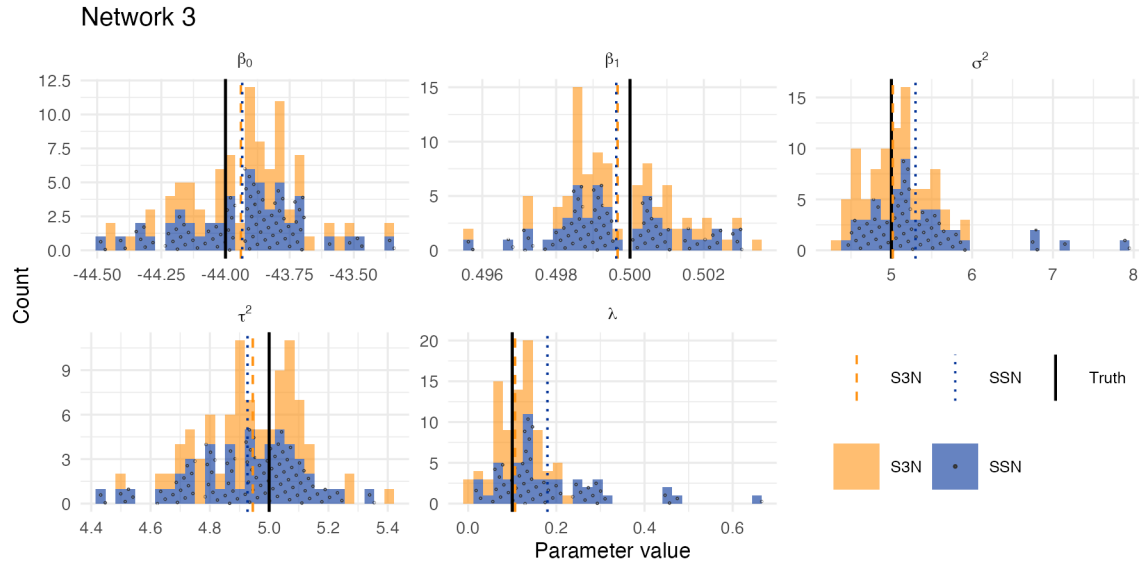


Figure 4: Model validation on Network 3. The solid black line indicates the true parameter values while the dashed and dotted lines represent the S3N and SSN averages, respectively, over 50 simulations. Both models are accurate and seem to be reasonably unbiased. Notably, S3N generally recovers the true stream covariance parameters σ^2 and λ better than SSN, even though the data were simulated from a full SSN.

3 against each other and against the true values, showing strong mutual agreement. Both models are accurate and appear reasonably unbiased. Both models improve with increasing network size, as expected since we simulated more observations for the larger networks. Interestingly, S3N generally recovers the true stream covariance parameters better than SSN despite the fact that the data were simulated from a full SSN, not a nearest-neighbor process. The distribution of the estimates of these covariance parameters tend to have a longer tail for the SSN model than for S3N, perhaps due to an accumulation of precision error.

4 Fish population estimates for the Ohio River Basin

We applied the S3N model to estimate the distributions and total population sizes for 285 species of fish across the entire Ohio River Basin, a dense river network comprising over 4,000 river km and an area of approximately 200,000 km², using observations at approximately 9,000 locations. This is the same stream network used in benchmarking as Network 6, the network on which SSN preprocessing crashed. The Ohio River Basin is one of the most species-rich river systems in North America. It includes diverse habitats—ranging from upland headwaters to large river channels—that support a wide variety of ecological niches and self-sustaining fish populations. Further details about the data and the analysis are available in the supplementary materials.

4.1 Fish survey data

In this study, we analyzed contemporary (1990–2023) fish community assemblage data (i.e., fish species counts) from 8,924 locations (stream segments) across the Ohio River Basin. This dataset is comprised of three national fish observation datasets—[Chen et al. \(2023\)](#), [Giam & Olden \(2016\)](#), and [Strecker et al. \(2011\)](#)—which themselves compile data from national and regional programs such as the United States Environmental Protection Agency (USEPA) Environmental Monitoring and Assessment Program (EMAP), the United States Geological Survey (USGS) National Water Quality Assessment Program (NAWQA), numerous state agency biomonitoring programs, and large-scale sampling efforts by other organizations and universities. Surveys were designed to accurately characterize species occurrence and abundance of fish species at each site. For this analysis, we limited sampling methods to standardized backpack or boat electrofishing, excluded records with unknown gear (likely duplicates), and retained only the most recent post-1990 observation for each species on each stream reach in the Ohio River Basin. Together, these datasets provide

the most comprehensive observations currently available, offering fish data that cover a large spatial extent but retain the fine spatial resolution necessary to evaluate fish species abundance at ecologically relevant scales.

To ensure that only comparable sampling events were analysed, we included only samples that used standardized electrofishing practices intended to characterize the entirety of stream fish community structure (Bonar et al. 2009). These are based on protocols designed to monitor stream fish communities uniformly across the US (Barbour et al. 1999, Moulton II et al. 2002). Surveys were designed to accurately characterize species occurrence and abundance of fish species at each site. All efforts involved sampling a defined stream reach length sufficient for characterizing local community structure, then identifying and enumerating all captured individuals. Fish are reported at the species level, and scientific names were harmonized according to FishBase using the `rfishbase` R package (Boettiger et al. 2012).

One challenge in modeling fish populations across large regions is the range in stream sizes. Isaak et al. (2017) used densities of fish per 100-m stream length instead of fish per water volume or per cross-sectional river area because they focus on larger fish in smaller streams. To account for this in our study, we assume the length of stream sampled within each survey was 20 times the mean bankfull channel width of the stream reach in which the sampling took place. We assumed a minimum and maximum stream length of 100 m and 1000 m, respectively, replacing the lengths of any sampling event that fell outside of this range. This is consistent with federal and most state fish monitoring electrofishing protocols (Hauer & Lamberti 2006). For the purposes of this study, the above protocol allows us to express the observed counts as densities by dividing each count by its corresponding estimated sampling length.

4.2 Environmental covariate data

We use nine environmental covariates to capture descriptions of watershed topography, land use, hydrology, and temperature, all key drivers of fish abundance ([Jackson et al. 2001](#)). Covariates include mean elevation (m); upstream watershed area (km^2); developed land cover (percentage of land with low, medium, or high development); agricultural land cover (percentage land used for pasture/hay or crops); total annual runoff (m^3 per year); mean annual air temperature (degrees Celsius); baseflow index; hydrological alteration index; and floodplain integrity. We use hydrological alteration index data and floodplain integrity data from [McManamay et al. \(2022\)](#) and [Morrison et al. \(2023\)](#), respectively, and all other variables are from the National Hydrography Dataset (NHD) Plus Version 2 Dataset (NHDPlus V2 data, model version 2.1, [Wieczorek et al. 2018](#)). In our region of interest, there were 806 missing values for hydrological alteration index and 299 for floodplain integrity, representing 0.48% and 0.18% of the stream network. We imputed these values by using the value from the nearest stream reach whose value was not missing.

4.3 Spatial model

Given observed fish densities $Y = (Y(s_1), \dots, Y(s_n))$ in fish per 100-m stream length at n point locations s_1, \dots, s_n across a region, we wish to estimate the geographic distribution of fish across the region and make regional population estimates by species. We fit a scalable

spatial stream network (S3N) model with an exponential tail-up covariance:

$$\begin{aligned}
Y &= X\beta + w, \quad w \sim N\left(0, \tilde{\Sigma}\right), \\
w(s_i) \mid w(M(s_i)) &\sim N(a_i, d_i), \\
a_i &= \Sigma(M(s_i), M(s_i))^{-1} \Sigma(M(s_i), s_i), \\
d_i &= \Sigma(s_i, s_i) - \Sigma(s_i, M(s_i)) a_i, \\
\Sigma(s_i, s_j) &= \pi_{ij} C_u(s_i, s_j \mid \theta_u) + \tau^2 \delta_{ij} \\
&= \pi_{ij} \sigma_u^2 \exp(-h(s_i, s_j)/\lambda_u) + \tau^2 \delta_{ij}.
\end{aligned} \tag{10}$$

We assume a normal distribution to model fish densities, and we show that this approach is sufficient and effective in this species-rich region, especially since we are ultimately interested in aggregating results over large regions. While this choice admits the possibility of negative predicted fish densities, we demonstrate in the next section that negative densities are exceedingly rare and small in magnitude, thus likely to correspond to areas truly lacking fish species. Before computing regional population estimates, we set negative densities to zero, so negative predicted densities are interpreted as an indication from the model that no or few fish are expected to be present in that location. Section 5 discusses potential future directions to extend this model to generalized linear models.

Preprocessing the entire stream network and computing pairwise stream distances can be done once for all 285 species, whereas estimation, inference, and prediction must be repeated for each species. Configuring the stream network was performed twice, once to assess the network for topological concerns and compute the network components, and again after refining the network to remove a complex confluence and restrict the network to the single largest component for simplicity. The vast majority (99.78%) of the network was retained as a result of this process.

Next, we computed the upstream distance and additive function value (a quantity used in

computing the spatial weights for the tail-up stream covariance) for each reach, mapped observation and prediction locations to the stream reaches, and computed their upstream distances and additive function values. After this preprocessing and before estimation, we computed the pairwise distances between observation points, and the pairwise distances between each prediction point and all observation points. We also identified the nearest neighbors of each observation point and each prediction point. In both cases, nearest neighbors were chosen among the observation locations only, since the purpose of these nearest neighbors is to use the observations to inform the model at observed and unobserved locations. These steps, particularly the prediction-observation pairwise distances, are highly parallelizable, so we computed the pairwise distances between prediction and observation points in 33 parallel batches of 5000 or fewer prediction points each.

For each species, we estimated model parameters using maximum likelihood estimation and estimated confidence intervals for both fixed effects and covariance parameters. To produce regional population size estimates for each species, we computed the predictive mean fish density per 100-m stream length at the midpoint of each stream reach, multiplied this by the length of the stream reach and by appropriate scale units to obtain an estimate for the mean number of fish in each stream reach, then summed across the reaches of the network to obtain a regional population estimate for that species. We use the estimated environmental fixed effects to examine the relationship between these variables and fish abundance.

We performed the entire analysis from preprocessing through prediction and visualization on a laptop (MacBook Pro 2020, 1.4 GHz Quad-Core Intel Core i5, 8 GB memory), with the exception of the pairwise distance calculations, which we ran on a research cluster.

4.4 Computational cost

Table 2 summarizes the runtimes for each step of the analysis. The time indicated for configuring the stream network, 2.1 minutes, includes initially configuring the network, identifying and removing the complex confluence, and reconfiguring the network. In total, the preprocessing took 3.8 minutes. Computing the pairwise distances among observations and between prediction and observation locations is currently the rate-limiting step of the S3N model, but these steps can be parallelized. Computing the observation pairwise distances and identifying nearest neighbors took 20 minutes. Computing the pairwise distances between prediction and observation points in 33 parallel batches took 26 minutes total.

Table 2: Runtimes for each step of the analysis. Preprocessing took 3.8 minutes, computing pairwise distances took 46 minutes, and estimation took 29 minutes (5.7 seconds per species).

Step	Runtime	
	In seconds	In minutes
Configure stream network	124	2.1
Compute stream updist and AFV	78	1.3
Add obs, preds to LSN	22	
Compute obs-obs dist on cluster	1190	20
Compute preds-obs dist on cluster	1580	26
Estimation, average per species	5.7	
Inference, average per species per rep	4.2	
Prediction, average per species	3.3	

Estimating model parameters and predicting fish densities across Region 5 took 5.7 and

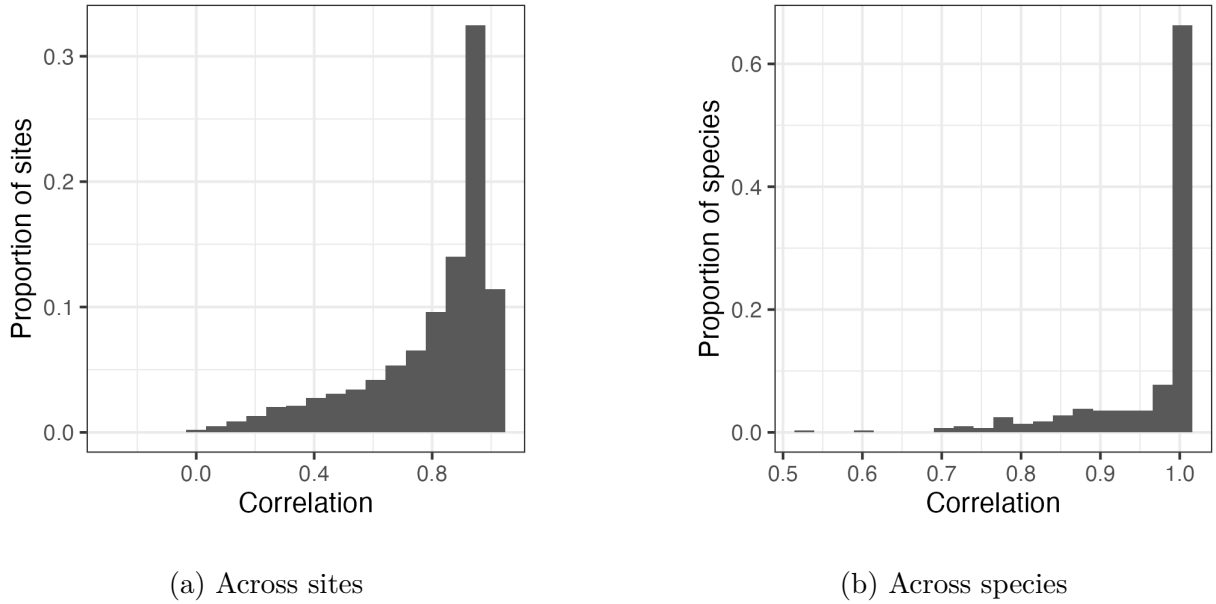


Figure 5: Correlations between predicted and observed densities (a) for each species across all sites and (b) at each site across all species.

3.3 seconds on average per species. Inference with the bootstrap takes approximately as long as estimation for each bootstrap replication (4.2 seconds). The total runtimes for estimation, inference and prediction for all 285 species with 20 bootstrap reps per species were 29 minutes, 438 minutes, and 17 minutes, respectively. If confidence intervals for the variance parameters are not of interest, only for the fixed effects, then the longest step—the bootstrap—can be omitted. Without the bootstrap, the total time for preprocessing, distance computation, estimation, and prediction is 1 hour 36 minutes for all 285 species, approximately 50 minutes for a single species.

4.5 Results

Model performance was strong at both the species and community levels. Species-level correlations between predicted and observed densities across sites ranged from 0.52 to 1.0 (mean = 0.96, SD = 0.19) (Figure 5a), while community-level correlations across species within each site averaged 0.80 (SD = 0.22), ranging from -0.29 to 1.0 (Figure 5b). The

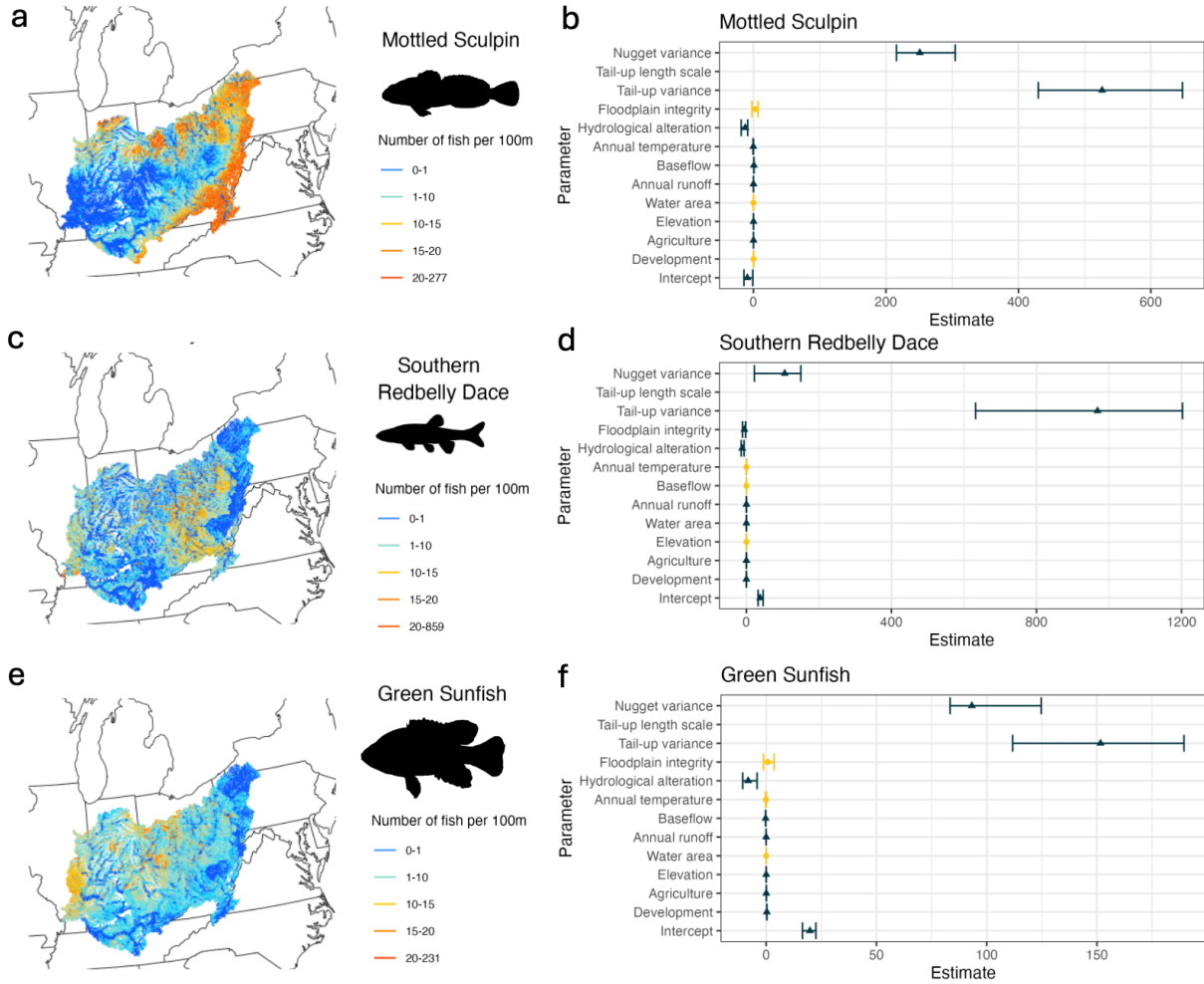


Figure 6: Maps of predictive mean fish density (fish per 100-m stream length), and estimates and confidence intervals of fixed effects and covariance parameters for three example species. Statistically significant coefficients are shown in dark blue with triangles for point estimates, while other coefficients are shown in yellow with circles for point estimates.

ratio of predicted to observed counts ranged from 0.2 to 1.02 at COMIDs where the species in question was observed, from 0.57 to 3.23 at COMIDs where any fish were observed, and from 1.2 to 120 for the entire region. These results offer support that model predictions were broadly consistent with the observed data.

The spatial distributions of predicted fish density for three example species—mottled sculpin (*Cottus bairdii*), southern redbelly dace (*Chrosomus erythrogaster*), and green sun-

fish (*Lepomis cyanellus*)—correspond with known distributions and dominant environmental drivers (Page and Burr 1991). Mottled sculpin in the Ohio River Basin is patchily distributed, occurring primarily in cool, clear, well-oxygenated streams of states such as Ohio, West Virginia, Pennsylvania, and Kentucky (Figure 6a), where it inhabits riffles and runs in upland streams with coarse substrates, while avoiding large, warm, or impacted rivers. This is supported by modeled densities that are negatively associated with annual temperature, annual discharge, and hydrologic alteration, and positively associated with elevation (Figure 6b). The Southern redbelly dace occurs primarily in small spring-fed or groundwater-influenced headwater streams that are cool, clear, shaded, and have gravel or sand substrates and abundant vegetation (Figure 6c). Dace populations have been extirpated in parts of their range where excessive siltation and turbidity are caused by the loss of forested lands, channelization and loss of lateral connectivity to the floodplain, and construction of dams that simplify river habitats; a finding supported by the strong negative association of density with developed and agricultural lands, hydrological alteration and floodplain disturbance (Figure 6d). The green sunfish is widespread throughout the basin (Figure 6e), occurring in a variety of warm, slow-flowing streams, reservoirs, and backwaters, and often thriving in disturbed or degraded habitats, as shown by modeled positive associations with developed and agricultural land (Figure 6f). These species examples demonstrate that the S3N model captures a range of geographic distributions and environmental determinants of freshwater fishes in the Ohio River Basin.

We note a small number of instances where the model predicted negative fish densities as a result of using a Gaussian process in the model. However, the mean proportion of segments predicted to have negative densities was just 0.0017 (or 0.17%) across species. Moreover, predicted negative densities are considerably smaller in magnitude when compared to predicted positive densities. Therefore, the small proportion of predicted negative densities

appear to correspond to locations and species for which the model predicts densities near zero.

5 Discussion

We introduce a scalable spatial stream network (S3N) model that enables estimation, inference, and prediction at a larger spatial scale and with greater computational efficiency than previously possible. S3Ns make spatial stream networks (SSNs) scalable by extending nearest-neighbor Gaussian processes (NNGPs) to include ecologically salient dependence structure and by incorporating more efficient preprocessing. We demonstrate that the S3N pipeline of preprocessing, estimation and prediction is feasible for the entire Ohio River Basin and even larger regions not yet attempted. Validation results indicate S3N correctly recovers parameter values, perhaps even with less bias and variance for spatial stream covariance parameters than current implementations of SSNs, despite having simulated the validation data from an SSN. The large-scale estimates presented here offer a critical step toward mapping the geographic distribution of freshwater fish species and understanding the role of environmental drivers at large scales.

Future work includes implementing tail-down and Euclidean covariance components, which require additional considerations. While covariates likely account for the majority of the Euclidean correlation and tail-up covariance captures stream correlations due to downstream flow, including these additional components would provide additional flexibility. For pairs of flow-unconnected points, tail-down covariance requires computing the distance from each point to their nearest common junction. Additionally, when both tail-up or tail-down and Euclidean covariances are included in the model, S3N models should ideally account for both the nearest neighbors with respect to Euclidean distance, $M_e(s_i)$, and those with respect to stream distance, $M_s(s_i)$. We can let $M(s_i) = M_e(s_i) \cup M_s(s_i)$. Ini-

tially, we could choose the m_e nearest neighbors with respect to Euclidean distance and the m_s nearest neighbors with respect to stream distance. An alternative is to choose the m_e nearest neighbors with respect to Euclidean distance and all observed locations that fall within some radius r_s with respect to stream distance.

Another direction for future work is to extend S3Ns to non-Gaussian distributions such as binomial, Poisson, zero-inflated Poisson, and negative binomial. This would better adapt S3Ns for modeling ecological count data. The adaptation of scalable spatial processes to generalized linear models is very recent. To our knowledge, [Finley et al. \(2022\)](#) developed the first and only NNGP application to use a non-Gaussian distribution, specifically the binomial distribution. Fixed-rank kriging, another approach to scalable spatial processes, only became adapted for non-Gaussian distributions in 2024 ([Sainsbury-Dale et al. 2024](#)).

It is also worth investigating the performance of different orderings of the point locations in defining the nearest neighbors. Under the full model without the nearest-neighbor approximation, the ordering does not matter. However, under the nearest-neighbor approximation, nearest neighbors are chosen only among the earlier points in the ordering, so the quality of the nearest-neighbor approximation depends on the index assigned to the locations ([Guinness 2018](#)). Future work should compare a few methods empirically and also explore theoretical arguments for using one method versus another.

Currently the slowest step in the current S3N implementation is computing the pairwise distances among observation points for estimation and prediction, and between prediction and observation points for prediction. This step can be made more efficient by using depth-first and breadth-first searches to first compute distances for the closest points and stop once the desired number of neighbors have been identified. In the future there are plans to make this change and to rewrite the code to minimize or eliminate use of `tidyverse` in favor of base R and C.

Thus far, we have applied the S3N model to the nearest-neighbor process to the responses, not the latent process which excludes the independent variance. This functionality could easily be added and is desirable if the independent variance is thought to arise solely from measurement error. While the computational savings over the full SSN model will not be as great for the latent process as for the response process, this option would enable users to make predictions at the latent level instead of the response level if they prefer.

In conclusion, this study introduces a scalable spatial stream network (S3N) model that enables larger-scale spatial process modeling on stream networks. By extending nearest-neighbor Gaussian processes to a stream-based context, identifying key preprocessing steps, and implementing them efficiently, we provide a framework capable of handling a computationally demanding task that limits the application of existing approaches. We demonstrate the utility of this approach through large-scale mapping of freshwater fish distributions and quantifying the influence of environmental drivers across broad networks. The S3N model represents a substantial advance in addressing the spatial dependence inherent in stream networks.

6 Disclosure statement

The authors have no conflicts of interest to declare.

7 Data and code availability

Covariate data used in this paper are publicly available. As mentioned above, we use hydrological alteration index data and floodplain integrity data from [McManamay et al. \(2022\)](#) and [Morrison et al. \(2023\)](#), respectively, and all other variables are from the National Hydrography Dataset (NHD) Plus Version 2 Dataset (NHDPlus V2 data, model version

2.1, [Wieczorek et al. 2018](#)).

The flowline and prediction point shapefiles from the National Stream Internet (NSI) are publicly available ([Nagel et al. 2017](#)).

Fish occurrence data were obtained through formal data sharing agreements with governmental agencies. As the respective agencies own these datasets, these data are not directly available for redistribution. Access to the raw data can be obtained through formal requests to the agencies listed in S1.

The code for estimation and prediction with S3N models is available through the `S3N` R package at <https://github.com/jpierkunke/S3N>.

The code to use the `S3N` package to reproduce the results of this paper is available at https://github.com/jpierkunke/S3N_paper.

Appendices

Section A describes the benchmarking results for comparing S3N and STARS, the older implementation of SSN preprocessing. Section B details how the steps of S3N and SSNbler were matched to each other for benchmarking purposes. Section C includes the validation results for Networks 1 and 2. Section D presents a list of agencies which provided fish occurrence data for the case study. Section E provides some additional details on the case study.

A Benchmarking against STARS

Since STARS is implemented in ArcGIS, we benchmarked it by adding timing steps to the Python scripts that constitute the STARS toolkit. Since STARS is less computationally efficient than the newer SSNbler, we limit our benchmarking of STARS to the first preprocessing step—building the stream network—and to a single network.

The Polyline to Landscape tool (hereafter PTL) of the STARS toolkit builds the stream network. The runtime of PTL on the Ohio River Basin stream network (Network 6 of the benchmarking networks) is approximately 4 hours. PTL has four main steps, whose names and runtimes are summarized in Table 3 along with the runtimes of the corresponding steps in S3N.

The first PTL step, called building hydro relationships, loops over stream reaches to extract the upstream and downstream nodes, adds these points with their coordinates to nodexy if they are not yet in the list, and creates a list of upstream nodes and a list of downstream nodes in the order in which the reaches are looped over, so that the i th upstream and downstream nodes correspond to the i th reach. This step took 24 minutes on the Ohio River Basin network (approximately Network 6). The analogous step in S3N is

PTL Step	Pre. Step	Runtime	
		PTL	S3N
Building Hydro Relationships	1a, 1b	24 min	1 min
Building Landscape Network Relationships	1c, 1d, 1e	3.3 hrs	0.5 sec
Sorting Relationship Table Downstream	NA	2 min	NA
Creating Landscape Network Features Classes	NA	17 min	NA

Table 3: Benchmarking results for the steps of the Polyline to Landscape (PTL) tool of the STARS toolkit, the preprocessing (Pre.) steps they correspond to, and the runtimes of S3N for those corresponding preprocessing steps. The fourth PTL step is required for their particular implementation but does not accomplish fundamentally required preprocessing steps, and there is no corresponding step in S3N; hence the preprocessing step and S3N runtime columns are NA for the last row of the table.

`add_upstream_dnstream_nodes()`, which takes approximately one minute (50-70 seconds) on the same network.

The second PTL step, building landscape network relationships, is the rate-limiting step. PTL loops over the list of downstream nodes which are one-to-one with the list of reaches, adds a row to a node relationships table to represent this reach and its upstream and downstream nodes, and then enters a second loop over all upstream nodes to determine which if any other reaches are directly downstream of the one in question. If so, then PTL adds an entry for each of these reaches to a relationships table. In a separate loop over reaches, the code determines which ones are sink reaches and adds them to a sink list. This step took 3.3 hours on the Ohio River Basin network. The analogous steps in S3N are `get_stream_graphs()` and `add_stream_source_outlet_component()`, which together take 0.4-0.8 seconds.

The third PTL step, sorting relationship table downstream, starts from each sink reach and works its way upstream in a loop, finding any and all reaches upstream of the current reach, adding those and the current reach as upstream and downstream nodes in new lists, deleting them from the old feature lists to reduce search time. PTL then loops through the network again to flip the order of these lists so that they are ordered downstream instead of upstream. This step is unnecessary once the stream adjacency matrix is computed, so there is no corresponding step in S3N. Instead, S3N starts at each sink and works its way upstream only when computing upstream distances and additive function values, and it computes them all in the same procedure. This step happens later in STARS preprocessing and we did not end up timing it because we started developing our own code once we knew that the earlier step of building the stream network was prohibitive.

The fourth PTL step, creating landscape network features classes, creates the points layer, copies various objects to the geodatabase, and stores and reformats results for their landscape network (LSN) object. These steps may be required for their particular implementation but they are not fundamentally required preprocessing steps, and there is no corresponding step in S3N. S3N similarly has its own implementation-specific additional steps which have no analogue in STARS/SSN, but the total runtime is much less than STARS/SSN.

B Benchmarking against `SSNbler`

Table 4 shows the model-to-model mapping we use for benchmarking.

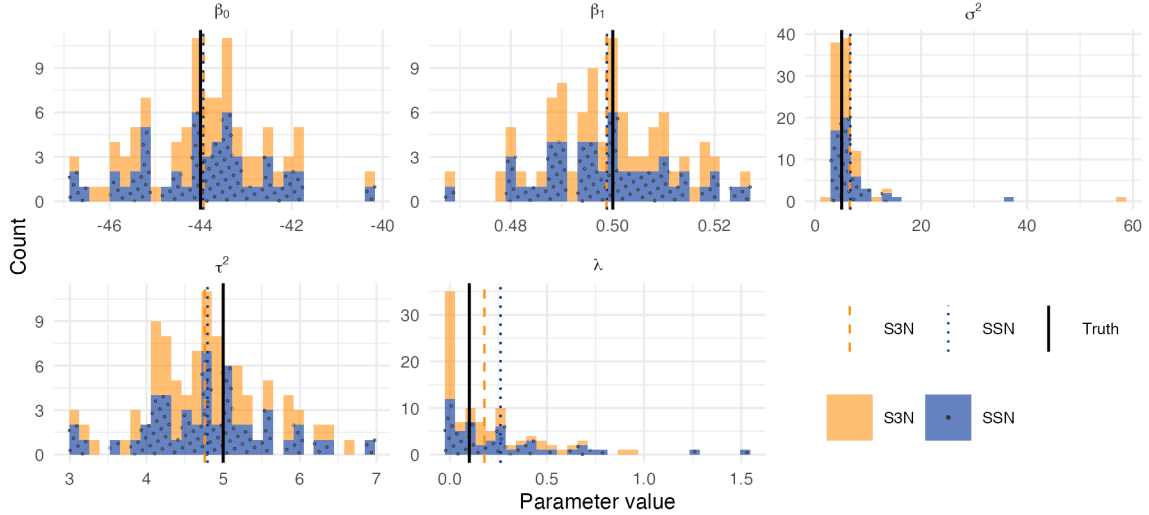
Task	S3N functions	SSN functions
Build stream network	<code>configure_stream_network()</code> - <code>add_upstream_dnstream_nodes()</code> - <code>get_stream_graphs()</code> - <code>add_stream_source_outlet_component()</code>	<code>lines_to_lsn()</code>
Compute stream updist	<code>compute_stream_updist_vars()</code>	<code>updist_edges()</code> <code>afv_edges()</code>
Compute site updist	<code>prep_to_compute_pwdist()</code>	<code>sites_to_lsn()</code> <code>updist_sites()</code> <code>afv_sites()</code>
Assemble SSN object	NA	<code>ssn_assemble()</code>
Compute pairwise distances	<code>compute_pwdists_preds_obs(obs_only = T)</code>	<code>ssn_create_distmat()</code>
Estimate model parameters	<code>BRISC_estimation_stream()</code>	<code>ssn_lm()</code>
Estimate CIs	<code>BRISC_bootstrap()</code>	NA

Table 4: Mapping S3N steps to SSN steps for benchmarking. Functions indented with a dash (-) are called by the function under which they are nested.

C Validation on Networks 1-2

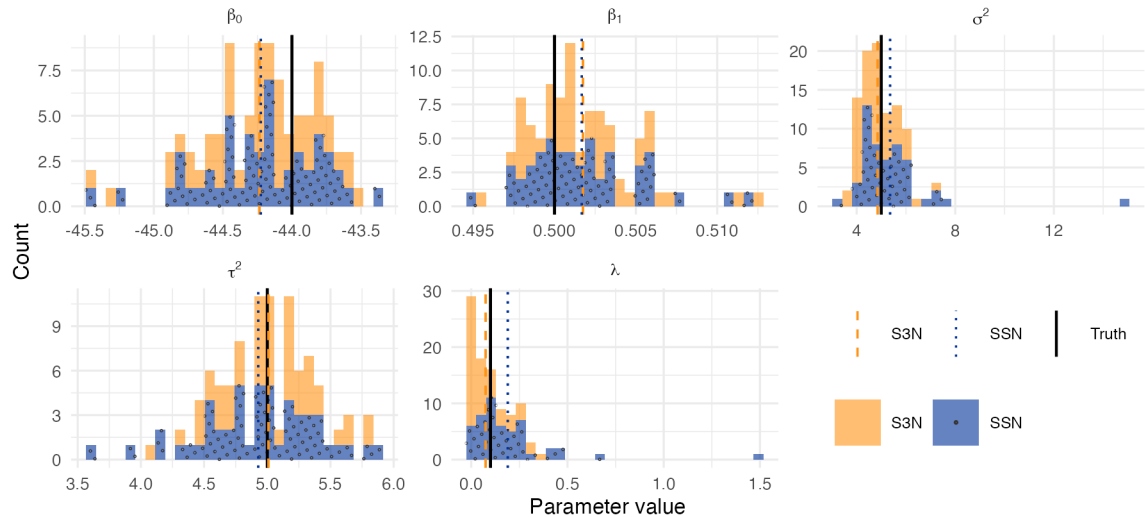
Validation results on Networks 1 and 2 were similar to those in Network 3. Recall that Network 1 had 284 reaches and 142 observation locations, Network 2 had 1,273 reaches and 634 observation locations, and Network 3 had 7,146 reaches and 3,562 observation locations. Observations were simulated from an SSN 50 times for each network, and each model (S3N and SSN) was fit once on each simulation. As expected, the bias and variance of both models reduce as the number of observations increases. In all three networks, the two models provide nearly equal estimates for the fixed effect parameters. However, in all three networks, S3N appears to provide more accurate estimates of the stream covari-

Network 1



(a)

Network 2



(b)

Figure 7: Validation results on Networks 1-2.

ance parameters. We are not sure yet whether this is due to less precision error or more regularization.

D Fish count data sources for the case study

Fish count data were obtained through formal data sharing agreements with governmental agencies. These data are not directly available for redistribution. Access to the raw data can be obtained through formal requests to the agencies and sources listed here.

- Giam and Olden (2016)
- Illinois Department of Natural Resources
- Indiana Department of Environmental Management
- Kentucky Energy and Environment Cabinet, Division of Water
- Maryland Department of Natural Resources
- New York Department of Environmental Conservation
- North Carolina Department of Environmental Quality, Biological Assessment Branch
- Ohio Environmental Protection Agency, Division of Surface Water, Standards and Technical Support Section
- Pennsylvania Department of Environmental Protection
- Susquehanna River Basin Commission
- Tennessee Wildlife Resources Agency
- Virginia Department of Environmental Quality
- West Virginia Department of Environmental Protection

E Further details about the case study

Each reach has a unique identifier called a COMID. Some of the environmental data are matched to stream locations by a different identifier, the hydrological unit code (HUC), so we match COMIDs to HUCs using a publicly available database. Of the 169,463 stream reaches in the NSI database for this region, 217 are short 20- to 40-meter segments that were added as part of their procedure to address gaps, complex confluences, and other topological errors or complexities incompatible with SSN models. These segments are assigned the same COMID as the neighboring reach directly upstream, which makes the COMID no longer a unique reach identifier. Therefore they add an additional field for each reach called the duplicate COMID to indicate whether the reach was added during this procedure (`DUP_COMID = 1`) or not (`DUP_COMID = 0`). To create a unique reach identifier, we reassign the COMID to a unique negative value for each reach with `DUP_COMID = 1` so that COMID is again unique. There is one complex confluence left in the network, so we remove the smallest upstream branch of the confluence, both the reach involved in the confluence and all nine reaches upstream of it. For simplicity in this initial analysis, we also select just the major connected component of the network, leaving us with 169,094 reaches or 99.78% of the NSI Region 5 network.

References

Altermatt, F. (2013), ‘Diversity in riverine metacommunities: a network perspective’, *Aquatic Ecology* **47**(3), 365–377.

Antonov, M., Csárdi, G., Horvát, S., Müller, K., Nepusz, T., Noom, D., Salmon, M., Traag, V., Welles, B. F. & Zanini, F. (2023), ‘igraph enables fast and robust network analysis across programming languages’, *arXiv preprint arXiv:2311.10260* .

Barbour, M. T., Gerritsen, J., Snyder, B. D. & Stribling, J. B. (1999), *Rapid bioassessment protocols for use in wadeable streams and rivers: periphyton, benthic macroinvertebrates and fish*, US Environmental Protection Agency, Office of Water.

Bilton, D. T., Freeland, J. R. & Okamura, B. (2001), 'Dispersal in freshwater invertebrates', *Annual review of ecology and systematics* **32**(1), 159–181.

Boettiger, C., Lang, D. T. & Wainwright, P. (2012), 'rfishbase: exploring, manipulating and visualizing fishbase data from r', *Journal of fish biology* **81**(6), 2030–2039.

Bonar, S. A., Hubert, W. A. & Willis, D. W. (2009), 'Standard methods for sampling north american freshwater fishes', *Standard methods for sampling North American freshwater fishes* .

Bond, N., Thomson, J., Reich, P. & Stein, J. (2011), 'Using species distribution models to infer potential climate change-induced range shifts of freshwater fish in south-eastern australia', *Marine and Freshwater Research* **62**(9), 1043.

Campbell Grant, E. H., Lowe, W. H. & Fagan, W. F. (2007), 'Living in the branches: population dynamics and ecological processes in dendritic networks', *Ecology Letters* **10**(2), 165–175.

Chen, K., Midway, S. R., Peoples, B. K., Wang, B. & Olden, J. D. (2023), 'Shifting taxonomic and functional community composition of rivers under land use change', *Ecology* **104**(11), e4155.

Comte, L. & Olden, J. D. (2018), 'Fish dispersal in flowing waters: A synthesis of movement- and genetic-based studies', *Fish and Fisheries* **19**(6), 1063–1077.

Cressie, N., Frey, J., Harch, B. & Smith, M. (2006), 'Spatial prediction on a river network', *Journal of Agricultural, Biological, and Environmental Statistics* **11**(2), 127–150.

Cressie, N. & Wikle, C. K. (2011), *Statistics for spatio-temporal data*, John Wiley & Sons.

Csárdi, G. & Nepusz, T. (2006), ‘The igraph software package for complex network research’, *InterJournal Complex Systems*, 1695.

Csárdi, G., Nepusz, T., Traag, V., Horvát, S., Zanini, F., Noom, D., Müller, K., Schoch, D. & Salmon, M. (2025), *igraph: Network Analysis and Visualization in R*. R package version 2.2.1.

Darwall, W., Bremerich, V., De Wever, A., Dell, A. I., Freyhof, J., Gessner, M. O., Grossart, H.-P., Harrison, I., Irvine, K., Jähnig, S. C., Jeschke, J. M., Lee, J. J., Lu, C., Lewandowska, A. M., Monaghan, M. T., Nejstgaard, J. C., Patricio, H., Schmidt-Kloiber, A., Stuart, S. N., Thieme, M., Tockner, K., Turak, E. & Weyl, O. (2018), ‘The alliance for freshwater life: A global call to unite efforts for freshwater biodiversity science and conservation’, *Aquatic Conservation: Marine and Freshwater Ecosystems* **28**(4), 1015–1022.

Datta, A. (2022), ‘Nearest-neighbor sparse cholesky matrices in spatial statistics’, *Wiley Interdisciplinary Reviews: Computational Statistics* **14**(5), e1574.

Datta, A., Banerjee, S., Finley, A. O. & Gelfand, A. E. (2016a), ‘Hierarchical nearest-neighbor Gaussian process models for large geostatistical datasets’, *Journal of the American Statistical Association* **111**(514), 800–812.

Datta, A., Banerjee, S., Finley, A. O. & Gelfand, A. E. (2016b), ‘On nearest-neighbor Gaussian process models for massive spatial data’, *Wiley Interdisciplinary Reviews: Computational Statistics* **8**(5), 162–171.

Dent, C. L. & Grimm, N. B. (1999), ‘Spatial heterogeneity of stream water nutrient concentrations over successional time’, *Ecology* **80**(7), 2283–2298.

Dumelle, M., Peterson, E. E., Ver Hoef, J. M., Pearse, A. & Isaak, D. J. (2024), ‘SSN2:

The next generation of spatial stream network modeling in R', *Journal of Open Source Software* **9**(99), 6389.

Erős, T., Olden, J. D., Schick, R. S., Schmera, D. & Fortin, M.-J. (2012), 'Characterizing connectivity relationships in freshwaters using patch-based graphs', *Landscape ecology* **27**(2), 303–317.

Fausch, K. D., Torgersen, C. E., Baxter, C. V. & Li, H. W. (2002), 'Landscapes to riverscapes: Bridging the gap between research and conservation of stream fishes', *BioScience* **52**(6), 483.

Finley, A. O., Datta, A. & Banerjee, S. (2022), 'spnngp r package for nearest neighbor gaussian process models', *Journal of Statistical Software* **103**, 1–40.

Ganio, L. M., Torgersen, C. E. & Gresswell, R. E. (2005), 'A geostatistical approach for describing spatial pattern in stream networks', *Frontiers in Ecology and the Environment* **3**(3), 138–144.

Giam, X. & Olden, J. D. (2016), 'Environment and predation govern fish community assembly in temperate streams', *Global Ecology and Biogeography* **25**(10), 1194–1205.

Guinness, J. (2018), 'Permutation and grouping methods for sharpening Gaussian process approximations', *Technometrics* **60**(4), 415–429.

Harper, M., Mejbel, H. S., Longert, D., Abell, R., Beard, T. D., Bennett, J. R., Carlson, S. M., Darwall, W., Dell, A., Domisch, S., Dudgeon, D., Freyhof, J., Harrison, I., Hughes, K. A., Jähnig, S. C., Jeschke, J. M., Lansdown, R., Lintermans, M., Lynch, A. J., Meredith, H. M. R., Molur, S., Olden, J. D., Ormerod, S. J., Patricio, H., Reid, A. J., Schmidt-Kloiber, A., Thieme, M., Tickner, D., Turak, E., Weyl, O. L. F. & Cooke, S. J. (2021), 'Twenty-five essential research questions to inform the protection and restoration

of freshwater biodiversity', *Aquatic Conservation: Marine and Freshwater Ecosystems* **31**(9), 2632–2653.

Hauer, F. R. & Lamberti, G. (2006), *Methods in stream ecology*, 2nd edn, Academic press.

Isaak, D. J., Peterson, E. E., Ver Hoef, J. M., Nagel, D., Wollrab, S., Chandler, G., Horan, D. & Parkes-Payne, S. (2020), 'Analysis of spatial stream networks for salmonids'.

Isaak, D. J., Ver Hoef, J. M., Peterson, E. E., Horan, D. L. & Nagel, D. E. (2017), 'Scalable population estimates using spatial-stream-network (SSN) models, fish density surveys, and national geospatial database frameworks for streams', *Canadian Journal of Fisheries and Aquatic Sciences* **74**(2), 147–156.

Jackson, D. A., Peres-Neto, P. R. & Olden, J. D. (2001), 'What controls who is where in freshwater fish communities – the roles of biotic, abiotic, and spatial factors', *Canadian Journal of Fisheries and Aquatic Sciences* **58**(1), 157–170.

Leibowitz, S. G., Wigington Jr., P. J., Schofield, K. A., Alexander, L. C., Vanderhoof, M. K. & Golden, H. E. (2018), 'Connectivity of streams and wetlands to downstream waters: An integrated systems framework', *JAWRA Journal of the American Water Resources Association* **54**(2), 298–322.

Lynch, A. J., Cooke, S. J., Arthington, A. H., Baigun, C., Bossenbroek, L., Dickens, C., Harrison, I., Kimirei, I., Langhans, S. D., Murchie, K. J., Olden, J. D., Ormerod, S. J., Owuor, M., Raghavan, R., Samways, M. J., Schinegger, R., Sharma, S., Tachamo-Shah, R., Tickner, D., Tweddle, D., Young, N. & Jähnig, S. C. (2023), 'People need freshwater biodiversity', *WIREs Water* **10**(3), e1633.

Markovic, D., Freyhof, J. & Wolter, C. (2012), 'Where are all the fish: Potential of biogeographical maps to project current and future distribution patterns of freshwater species', *PLoS ONE* **7**(7), e40530.

McManamay, R. A., George, R., Morrison, R. R. & Ruddell, B. L. (2022), 'Mapping hydrologic alteration and ecological consequences in stream reaches of the conterminous United States', *Scientific Data* **9**(1), 450.

Morrison, R. R., Simonson, K., McManamay, R. A. & Carver, D. (2023), 'Degradation of floodplain integrity within the contiguous United States', *Communications Earth & Environment* **4**(1), 215.

Moulton II, S. R., Kennen, J., Goldstein, R. M. & Hambrook, J. A. (2002), Revised protocols for sampling algal, invertebrate, and fish communities as part of the national water-quality assessment program, Technical report, Geological Survey (US).

Nagel, D., Wollrab, S., Parkes-Payne, S., Peterson, E., Isaak, D. & Ver Hoef, J. (2017), National Stream Internet hydrography datasets for spatial-stream-network (SSN) analysis, Technical report, Rocky Mountain Research Station, US Forest Service Data Archive, Fort Collins, CO.

Olden, J. D., Kennard, M. J., Leprieur, F., Tedesco, P. A., Winemiller, K. O. & García-Berthou, E. (2010), 'Conservation biogeography of freshwater fishes: recent progress and future challenges', *Diversity and Distributions* **16**(3), 496–513.

Olea, R. A. & Pardo-Igúzquiza, E. (2011), 'Generalized bootstrap method for assessment of uncertainty in semivariogram inference', *Mathematical Geosciences* **43**, 203–228.

Paukert, C., Olden, J. D., Lynch, A. J., Breshears, D. D., Christopher Chambers, R., Chu, C., Daly, M., Dibble, K. L., Falke, J., Issak, D., Jacobson, P., Jensen, O. P. & Munroe, D. (2021), 'Climate change effects on north american fish and fisheries to inform adaptation strategies', *Fisheries* **46**(9), 449–464.

Pebesma, E. (2018), 'Simple Features for R: Standardized Support for Spatial Vector Data',

The R Journal **10**(1), 439–446.

URL: <https://doi.org/10.32614/RJ-2018-009>

Pebesma, E. & Bivand, R. (2023), *Spatial Data Science: With applications in R*, Chapman and Hall/CRC.

URL: <https://r-spatial.org/book/>

Peterson, E., Dumelle, M., Pearse, A., Teleki, D. & Ver Hoef, J. M. (2024), *SSNbler: Assemble SSN objects in R*, R package version 1.1.0.

Peterson, E. E., Merton, A. A., Theobald, D. M. & Urquhart, N. S. (2006), ‘Patterns of spatial autocorrelation in stream water chemistry’, *Environmental Monitoring and Assessment* **121**, 571–596.

Peterson, E. & Ver Hoef, J. (2014), ‘STARS: An ArcGIS toolset used to calculate the spatial information needed to fit spatial statistical models to stream network data’, *Journal of Statistical Software* **56**, 1–17.

Radinger, J., Essl, F., Hölker, F., Horký, P., Slavík, O. & Wolter, C. (2017), ‘The future distribution of river fish: The complex interplay of climate and land use changes, species dispersal and movement barriers’, *Global Change Biology* **23**(11), 4970–4986.

Rasmussen, C. E. & Williams, C. K. (2006), *Gaussian Processes for Machine Learning*, MIT press, Cambridge, MA.

Reid, A. J., Carlson, A. K., Creed, I. F., Eliason, E. J., Gell, P. A., Johnson, P. T., Kidd, K. A., MacCormack, T. J., Olden, J. D., Ormerod, S. J. et al. (2019), ‘Emerging threats and persistent conservation challenges for freshwater biodiversity’, *Biological reviews* **94**(3), 849–873.

Rogosch, J. S., Tonkin, J. D., Lytle, D. A., Merritt, D. M., Reynolds, L. V. & Olden, J. D.

(2019), ‘Increasing drought favors nonnative fishes in a dryland river: evidence from a multispecies demographic model’, *Ecosphere* **10**(4), e02681.

Saha, A. & Datta, A. (2018), ‘BRISC: Bootstrap for rapid inference on spatial covariances’, *Stat* **7**(1), e184.

Sainsbury-Dale, M., Zammit-Mangion, A. & Cressie, N. (2024), ‘Modeling big, heterogeneous, non-gaussian spatial and spatio-temporal data using *frk*’, *Journal of Statistical Software* **108**, 1–39.

Schofield, K. A., Alexander, L. C., Ridley, C. E., Vanderhoof, M. K., Fritz, K. M., Autrey, B. C., DeMeester, J. E., Kepner, W. G., Lane, C. R., Leibowitz, S. G. & Pollard, A. I. (2018), ‘Biota connect aquatic habitats throughout freshwater ecosystem mosaics’, *JAWRA Journal of the American Water Resources Association* **54**(2), 372–399.

Stein, M. L. (2014), ‘Limitations on low rank approximations for covariance matrices of spatial data’, *Spatial Statistics* **8**, 1–19.

Strecker, A. L., Olden, J. D., Whittier, J. B. & Paukert, C. P. (2011), ‘Defining conservation priorities for freshwater fishes according to taxonomic, functional, and phylogenetic diversity’, *Ecological Applications* **21**(8), 3002–3013.

Tickner, D., Opperman, J. J., Abell, R., Acreman, M., Arthington, A. H., Bunn, S. E., Cooke, S. J., Dalton, J., Darwall, W., Edwards, G., Harrison, I., Hughes, K., Jones, T., Leclère, D., Lynch, A. J., Leonard, P., McClain, M. E., Muruven, D., Olden, J. D., Ormerod, S. J., Robinson, J., Tharme, R. E., Thieme, M., Tockner, K., Wright, M. & Young, L. (2020), ‘Bending the curve of global freshwater biodiversity loss: An emergency recovery plan’, *BioScience* **70**(4), 330–342.

Tonkin, J. D., Altermatt, F., Finn, D. S., Heino, J., Olden, J. D., Pauls, S. U. & Lytle, D. A.

(2018), 'The role of dispersal in river network metacommunities: Patterns, processes, and pathways', *Freshwater Biology* **63**(1), 141–163.

Tonkin, J. D., Olden, J. D., Merritt, D. M., Reynolds, L. V., Rogosch, J. S. & Lytle, D. A. (2021), 'Designing flow regimes to support entire river ecosystems', *Frontiers in Ecology and the Environment* **19**(6), 326–333.

Urban, M. C. (2024), 'Climate change extinctions', *Science* **386**(6726), 1123–1128.

Vannote, R. L., Minshall, G. W., Cummins, K. W., Sedell, J. R. & Cushing, C. E. (1980), 'The river continuum concept', *Canadian journal of fisheries and aquatic sciences* **37**(1), 130–137.

Vecchia, A. V. (1988), 'Estimation and model identification for continuous spatial processes', *Journal of the Royal Statistical Society Series B: Statistical Methodology* **50**(2), 297–312.

Ver Hoef, J. M. & Barry, R. P. (1996), 'Constructing and fitting models for cokriging and multivariable spatial prediction', *Journal of Agricultural, Biological, and Environmental Statistics* **1**(3), 297–322.

Ver Hoef, J. M. & Peterson, E. E. (2010), 'A moving average approach for spatial statistical models of stream networks', *Journal of the American Statistical Association* **105**(489), 6–18.

Ver Hoef, J. M., Peterson, E. E. & Isaak, D. J. (2019), Spatial statistical models for stream networks, in A. E. Gelfand, M. Fuentes, J. A. Hoeting & R. L. Smith, eds, 'Handbook of Environmental and Ecological Statistics', Chapman and Hall/CRC, pp. 421–444.

Ver Hoef, J. M., Peterson, E. & Theobald, D. (2006), 'Spatial statistical models that use flow and stream distance', *Environmental and Ecological statistics* **13**, 449–464.

Ver Hoef, J., Peterson, E., Clifford, D. & Shah, R. (2014), 'SSN: An R package for spatial statistical modeling on stream networks', *Journal of Statistical Software* **56**, 1–45.

Wagner, T., Hansen, G. J., Schliep, E. M., Bethke, B. J., Honsey, A. E., Jacobson, P. C., Kline, B. C. & White, S. L. (2020), 'Improved understanding and prediction of freshwater fish communities through the use of joint species distribution models', *Canadian Journal of Fisheries and Aquatic Sciences* **77**(9), 1540–1551.

Webster, R. A., Pollock, K. H., Ghosh, S. K. & Hankin, D. G. (2008), 'Bayesian spatial modeling of data from unit-count surveys of fish in streams', *Transactions of the American Fisheries Society* **137**(2), 438–453.

Wieczorek, M., Jackson, S. & Schwarz, G. (2018), 'Select attributes for NHDPlus version 2.1 reach catchments and modified network routed upstream watersheds for the conterminous United States', *US Geological Survey* **10**, F7765D7V.

Wyatt, R. J. (2003), 'Mapping the abundance of riverine fish populations: integrating hierarchical Bayesian models with a geographic information system (GIS)', *Canadian Journal of Fisheries and Aquatic Sciences* **60**(8), 997–1006.

Yaglom, A. (1987), *Correlation Theory of Stationary and Related Random Functions*, Springer.